Carbohydrate Polymers 90 (2012) 87–94

Contents lists available at SciVerse ScienceDirect

Carbohydrate Polymers

journal homepage: www.elsevier.com/locate/carbpol

Oxidation of crosslinked chitosan-epichlorohydrine film and its application with TiO_2 for phenol removal

Ali H. Jawad, M.A. Nawi*

School of Chemical Sciences, Universiti Sains Malaysia, 11800 Pulau Penang, Malaysia

ARTICLE INFO

Article history:
Received 8 February 2012
Received in revised form 23 April 2012
Accepted 27 April 2012
Available online 5 May 2012

Keywords:
Chitosan
Epichlorohydrin
Crosslinking
Photocatalysis
Oxidation
Phenol

ABSTRACT

Photocatalytic oxidation of crosslinked chitosan-epichlorohydrin (CS-ECH) film was successfully achieved via an immobilized TiO_2/CS-ECH photocatalyst system on a glass plate. Oxidation process of CS-ECH film was carried out by irradiating the system with a 45-W fluorescent lamp for 10 h in ultra-pure water. The results indicate the formation of carbonyl functional groups and partial elimination of amine groups in the molecular structure of the oxidized CS-ECH film. This oxidized CS-ECH film has different optical properties, ionic conductivity, degree of transparency, swelling index and chemical stability than the fresh CS-ECH film. In the environmental applications, the TiO_2/oxidized-CS-ECH photocatalyst system can have photodegradation and faster mineralization rate of phenol than both fresh TiO_2/CS-ECH and TiO_2/oxidized-CS photocatalyst systems. This simple photocatalyst system, therefore can be considered as an environmental friendly method to oxidize synthetic biopolymer and to improve the photocatalytic efficiency of TiO_2 to treat wastewater.

1. Introduction

In the recent decades, development of natural cost effective biopolymer has gained a prime position in the polymer processing technology. Chitosan (CS) (β-(1–4)-2-amino-2-deoxy-D-glucose) is an abundant cycloaliphatic biopolymer derived from the deacetylation of the naturally occurring biopolymer chitin (β-(1–4)-2-acetamido-2-deoxy-D-glucose) which is considered as the second most abundant polysaccharide in the world after cellulose (Crini & Badot, 2008). The amino (—NH_2) and hydroxyl (—OH) groups on its polymeric chain can act as adsorption sites for removing pollutants from wastewater (Chang & Juang, 2004) and also as reaction sites for chemical modification by several crosslinking agents (Kumar, 2000). Physical modification of CS can be achieved by protonation of the amino functional group on the C-2 position of the D-glucosamine repeating unit, which causes the dissolution of the CS biopolymer in acidic solutions (Kumar, 2000). This CS can be converted into various forms such as gel beads (Ngah, Ghani, and Hoon, 2002; Ngah, Endud, & Mayanar, 2002), hollow fibers (Blondet, Vincent, & Guibal, 2008), sponge-like (Mi et al., 2001), membrane (Wan, Creber, Peppley, & Bui, 2003) and thin layer (Nawi, Sabar, Jawad, & Ngah, 2010) in order to meet the requirements of the many applications in different fields.

The chemical modification of CS by using crosslinking reaction offers an alternative pathway for producing chemically more stable CS's derivatives, which can extend the potential applications of this biopolymer to more areas. In this respect, blocking the hydrophilic amino (—NH_2) and hydroxyl (—OH) groups in the CS backbone with the commonly used crosslinking agents of glutaraldehyde (GLA) and epichlorohyrine (ECH) respectively leads to improve pore size distribution, chemical stability, mechanical resistance and adsorption/desorption properties (Baroni, Vieira, Meneghetti, da Silva, & Beppu, 2008).

The photo-modification of CS can be considered as a fast and convenient way for producing high purity CS's oligomers without using initiator, oxidizing agents and/or complex experimental procedures. These CS's oligomers have lower molecular weight and viscosity, and higher water-solubility due to the breaking of the β-D-(1 → 4) glycosidic bonds between the two repeat units of CS (Choi, Ahn, Lee, Byun, & Park, 2002). Photocatalysis can also modify CS without breaking it down into its oligomeric forms. In our previous work (Nawi, Jawad, Sabar, & Ngah, 2011a), a solid state natural CS had been successfully oxidized by using a simple assemblage of the bilayer TiO_2/CS system under irradiation of indoor fluorescent lamp. This alternative environmental friendly method facilitates the formation of the chemically more stable and optically active form of the oxidized CS without altering much of its polymeric structure. In addition, following studies showed that the TiO_2/oxidized-CS photocatalyst system had better photocatalytic performance than fresh TiO_2/CS, slurry TiO_2 and immobilized TiO_2 photocatalyst systems for the removal of phenol (Nawi, Jawad, Sabar, & Ngah, 2011b), and its intermediates (Jawad & Nawi, 2011).

These interesting findings inspired us to move forward for modifying crosslinked biopolymer by using heterogeneous TiO_2

* Corresponding author. Tel.: +60 4 6534031; fax: +60 4 6574854.
E-mail addresses: ahjm72@yahoo.com (A.H. Jawad), masri@usm.my (M.A. Nawi).

0144-8617/$ – see front matter © 2012 Elsevier Ltd. All rights reserved.
http://dx.doi.org/10.1016/j.carbpol.2012.04.066

photocatalyst technology for better physicochemical and optical properties. In fact, adding carbonyl (C=O) functional groups onto the polymeric structure of the crosslinked biopolymer can enhance many of the physicochemical properties related to the optical properties, opacity (degree of transparency), ionic conductivity, hydrophobicity and chemical stability. Producing multifunctional biomaterials with different physicochemical properties may be useful for extending their potential applications in the areas of water treatment technology, biosensors, membrane, adhesive, hydrogels, drug delivery, tissue engineering and other biomedical applications.

Therefore, the first objective of this work was to oxidize a crosslinked chitosan-epichlorohydrine (CS-ECH) film by using heterogeneous TiO_2 photocatalyst technology so that new physicochemical properties can be generated for that synthetic biomaterial. The second objective was to investigate the effect of the oxidized CS-ECH film on the photocatalytic performance of TiO_2 photocatalyst in the water treatment technology by combining them in the form of immobilized TiO_2/oxidized-CS-ECH photocatalyst system. Phenol was chosen as the model pollutant in evaluating the photocatalytic performance of the photocatalyst system because of the negligible adsorptive effect of phenol by the system. Moreover, the complication from the adsorption-photocatalysis synergistic effect as normally observed in the removal of dyes (Li, Su, & Tan, 2008; Zainal, Hui, Hussein, Abdullah, & Hamadneh, 2009; Zubieta et al., 2008) can be avoided in this work. Hence, the immobilization of the photocatalyst system can effectively overcome the post-treatment catalyst powder recovery and the difficulty of filtration or separation processes.

2. Materials and methods

2.1. Chemicals

CS of medium molecular weight of 322 g mol^{-1} with a 68.20% degree of deacetylation as determined by infrared spectroscopy method (Kasaai, 2008) was purchased from Sigma–Aldrich. ECH (≥98% (w/v) aqueous solution) was supplied by Fluka. Titanium(IV) oxide (99% anatase) was obtained from Sigma–Aldrich. Phenol-formaldehyde powder resin (PF) was bought from Borden Chemical Sdn. Bhd., Malaysia. Epoxidized natural rubber (ENR50) was obtained from Kumpulan Guthrie Sdn. Bhd., Malaysia. All the materials were used as received without further purification. Ultrapure water (18.2 MΩ cm^{-1}) was used in this work.

2.2. Fabricating of TiO_2/CS-ECH photocatalyst system

Fabrication of the immobilized TiO_2/CS-ECH photocatalyst system involved two main steps:

(a) Crosslinking and casting of CS-ECH: The crosslinking reaction followed the procedure described by Ngah, Ghani, et al. (2002) and Ngah, Endud, et al. (2002) with some modifications. 2.0 g of CS flakes were dissolved in 90 mL of 5% (v/v) acetic acid solution. The viscous solution of CS was left for more than 24 h with vigorous stirring to ensure that all of the CS flakes were completely dissolved. The obtained gel of CS was filtered through polystyrene sieve, and then 85 mL of 0.05 M ECH was added into this gel with gentle stirring for 1 h to obtain a ratio of 1:1 (mol CH_2O:mol CH_2OH), the CH_2O was from ECH, and the CH_2OH was from the CS solution. The bubbles-free homogeneously crosslinked CS-ECH gel (colorless and transparent) was evenly casted onto a glass plate of dimension 4.7 cm × 6.5 cm and allowed to dry for 5 days in order to produce an immobilized colorless and transparent crosslinked CS-ECH film. This immobilized CS-ECH film was rinsed several times with water to remove any trace of HCl formed as a by-product during the crosslinking reaction and dried at room temperature. Thickness of CS-ECH film obtained by casting 0.65 ± 0.08 mg cm^{-2} of CS-ECH solution onto a glass plate measured by SEM microscope (image not shown) was found to be 4.81 ± 0.07 μm.

(b) TiO_2 formulation and coating technique: The photocatalyst formulation was prepared by adding fixed amounts of 0.15 g phenol-formaldehyde resin (PF) as an adhesive co-agent and 5 g epoxidized natural rubber (ENR50) solution (11.32% solution of ENR50 in toluene) as a binder into an amber bottle which contained 12 g TiO_2 powder. Finally, 60 mL of acetone was poured into the bottle before being homogenized by sonication for 5 h. The TiO_2 formulation was deposited onto CS-ECH film by using a simple dip-coating method. This method involved dipping and drying processes of the immobilized CS-ECH film into TiO_2 formulation until the desired amount of TiO_2 was fixed on top of the CS-ECH film. The thickness of the TiO_2 layer obtained by deposition of 1.30 ± 0.08 mg cm^{-2} of TiO_2 was 40.94 ± 1.16 μm.

2.3. Photocatalytic oxidation of CS-ECH film

The irradiation process for the immobilized TiO_2/CS-ECH photocatalyst system was carried out in the presence of the ultra-pure water, air and in ambient conditions of pH 6.6 and temperature 25 °C throughout this work. The immobilized TiO_2/CS-ECH photocatalyst system was placed upright inside a homemade photo-reactor cell of dimension 5 cm × 8 cm × 1 cm, and then filled-up with 20 mL of ultra-pure water. The air was supplied by using an aquarium air pump with a constant aeration flow rate at 25 mL min^{-1}. Finally, a 45-W compact household fluorescent lamp with UV leakage of 4.4 Wm^{-2} was placed directly in front of the outer side of the photo-reactor cell.

2.4. Physicochemical characterizations of CS-ECH film

All physicochemical characterizations of the CS-ECH films were carried out by removing this film manually from the glass plate by using a razor blade. While, for the irradiated CS-ECH film in the TiO_2/CS-ECH photocatalyst system, the TiO_2 top layer was firstly removed by intensive rinsing with acetone and brushing with a laboratory brush until the entire TiO_2 layer was visually gone. It was then followed by rinsing with ultra-pure water and left to dry at room temperature and finally the clean irradiated CS-ECH film was carefully removed from the glass plate using a razor blade as described above. The elemental analysis was carried out by using CHN analyzer (Perkin-Elmer, Series II, 2400). FTIR spectra were obtained via a Perkin-Elmer Fourier-transform infrared spectroscopy system (spectrum BX). The solid state ^{13}C nuclear magnetic resonance (^{13}C NMR) spectra were recorded by using spectrophotometer (BRUKER, AVANCE 400) combining cross polarization (CP) and magic-angle spinning (MAS) techniques at a spinning rate of 8 kHz and frequency 100 Hz where the samples were ground and packed into zirconia rotors (length: 2 cm; internal diameter: 5 mm). Diffuse reflectance UV–visible spectroscopy (UV–vis DRS) were carried out on a Perkin-Elmer, Lambda 35 UV–vis spectrometer. Photoluminescence spectra (PL) were recorded by using Raman & Photoluminescence spectroscopy system (model: Jobin Yvon HR 800 UV). The potentiometric titration was performed according to the published method of Vieira and Beppu (2006) by using a pH meter (Metrohm, 827 pH lab). The swelling index (SI) was also calculated according to the procedure described by Wan et al. (2003). The impedance (R) spectroscopy measurement was performed and the ionic conductivity was calculated according to the published method (Rodrigues, Forte, Azambuja, & Castagno, 2007) by using precision impedance

Fig. 1. The photographs of (a) fresh CS-ECH film and (b) oxidized CS-ECH film. (For interpretation of the references to color in text, the reader is referred to the web version of this article.)

analyzer (Agilent 4294A). The UV leakage of the 45-W compact household fluorescent lamp was determined through a radiometer (Solar light co. PMA 2100) connected with a UV-A and UV-B broadband detector (PMA 2107). The aeration flow rate was maintained at 25 mL min^{-1} throughout this work by using a Gilmont direct reading flow meter.

2.5. Application of TiO_2/CS-ECH photocatalyst system for phenol removal

The photocatalytic performances of the fresh TiO_2/CS-ECH photocatalyst system and TiO_2/oxidized-CS-ECH photocatalyst system were evaluated for removal of 20 mL of 10 mg L^{-1} phenol by applying the same experimental set-up as mentioned in Section 2.3. The kinetics of degraded phenol by all the photocatalytic systems and chemical oxygen demand (COD) analysis were carried out according to the published procedures (Nawi et al., 2011b).

3. Results and discussion

3.1. Physicochemical characterizations

Oxidation of CS-ECH film was carried out by irradiating the TiO_2/CS-ECH system for 10 h in ultra-pure water. During the irradiation process, development of macro-pores on the TiO_2 surface take place due to the photodegradation of a considerable part of the ENR_{50} binder (Nawi et al., 2011b). The diffusion of hydroxyl radicals from the surface of TiO_2 toward the interface of the TiO_2/CS-ECH layers could occur through these generated macro-pores. Consequently, the hydroxyl radicals were considered to be responsible for the oxidation of CS-ECH film. The characterizations on the CS-ECH film before and after the photocatalytic oxidation process are summarized below.

3.1.1. Change in visual color

Fig. 1(a) and (b) shows the photographs of the fresh and oxidized CS-ECH film respectively. The visual color and the degree of transparency of the CS-ECH film has totally changed from colorless and transparent to deep brown color after the irradiation process. The color transformation in this case can be attributed to the formation of carbonyl chromophore group in the polymeric structure of the oxidized CS-ECH film. In this respect, a number of works had observed that brownish color of biopolymers can be obtained by photo-oxidation of polysaccharides such as chitosan (Choi et al., 2002; Nawi et al., 2011a; Zainol, Akil, & Mastor, 2009) and sodium alginate (Nagasawa, Mitomo, Yoshii, & Kume, 2000).

3.1.2. Diffuse reflectance UV–visible spectroscopy (DRS) analysis

To confirm the above presumption, the UV–vis DRS spectra of fresh and oxidized CS-ECH film are shown in Fig. 2(a) and (b) respectively. An absorption band around 220 nm is clearly observed in spectrum (a) which can be assigned to the $n \rightarrow \sigma^*$ transition for the amine groups of CS (Wang, Huang, & Wang, 2005). On the other hand, spectrum (b) shows a remarkable decrease in the absorption band 220 nm which can be attributed to the partial elimination of the amine groups. At the same time, a clear red-shift toward longer wavelength corresponding to a new spectral absorption band around 360 nm can be clearly seen. This absorption band can be attributed to the $n \rightarrow \pi^*$ transition for the newly formed carbonyl chromophore group in the molecular structure of the irradiated CS-ECH film. Based on the data reported in the published literature (Andrady, Torikai, & Kobatake, 1996; Nagasawa et al., 2000;

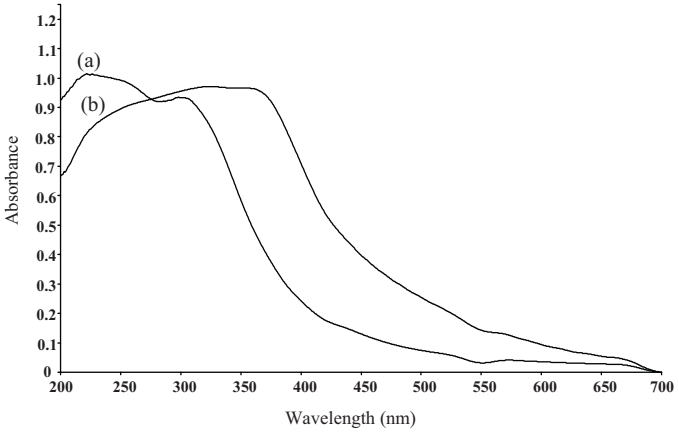

Fig. 2. UV–vis DRS spectra of (a) fresh CS-ECH film and (b) oxidized CS-ECH film.

Nawi et al., 2011a; Wang et al., 2005) the formation of the carbonyl chromophore groups by the photo-oxidation treatment of polysaccharides are basically responsible for the appearance of a new absorption band in the UV–vis spectrum.

3.1.3. Photoluminescence (PL) analysis

Photoluminescence analysis shows that the emission intensity of the fresh CS-ECH film is significantly reduced after irradiation, as shown in Supplementary Fig. 1. This remarkable reduction in the emission intensity can be attributed to the formation of an electron-withdrawing carbonyl (C=O) functional group in the molecular structure of the oxidized CS-ECH film. The low photoluminescence yield of the primary $n \rightarrow \pi^*$ transition of the carbonyl functional group is the reason why spectrum (b) exhibits lower emission intensity than spectrum (a) (Levin, 2003).

3.1.4. Potentiometric titrations

The potentiometric titrations were carried out in order to determine quantitatively the percentage of amino groups in the chemical structure of the CS-ECH film before and after photocatalytic oxidation process. The obtained results were summarized in Table 1. It was found that the oxidized CS-ECH film had significantly lower percentage (32%) of amino groups than fresh CS-ECH film. This means that the average number of protons bound to the free amino groups in the chemical structure of the irradiated CS-ECH film became less due to the partial elimination of the amino groups during the photocatalytic oxidation process.

3.1.5. Swelling index

Swelling test was performed in order to compare the swelling behavior of the fresh CS-ECH film and oxidized CS-ECH film. It was found that the oxidized CS-ECH film had lower swelling index than the fresh CS-ECH film as summarized in Table 1. This decrease in swelling index could be attributed to the lesser content of amino groups remaining in the oxidized CS-ECH film as determined previously by the potentiometric titration measurement. Consequently, the polymeric structure of the irradiated CS-ECH film had become more hydrophobic.

3.1.6. Ionic conductivity measurement

The results obtained from the impedance measurements were converted to the corresponding ionic conductivity values as summarized in Table 1. The oxidized CS-ECH film showed lower bulk impedance and higher ionic conductivity than the fresh CS-ECH film. This phenomenon is basically due to the formation of the carbonyl functional group in the polymeric structure of the oxidized CS-ECH film. In fact, the formation of the carbonyl group as an additional functional group could be responsible for increasing the mobility of the structural network and the density of the potential charge carriers. Therefore, better ionic conductivity was obtained from the photo-modified biopolymer.

3.1.7. CHN analysis

The elemental content of the fresh and oxidized CS-ECH films are given in Table 1. The mass ratio of C/N of the oxidized CS-ECH film was remarkably decreased which indicated the occurrence of partial elimination of some amino groups. The minor increase in mass ratio of C/H could be attributed to the oxidation process of hydroxyl groups at C-3 of the repetitive pyranose units of CS into a carbonyl group with the loss of the hydrogen atoms. It has been reported that the irradiation of CS derivatives led to partial elimination of some amino groups which corresponded with the higher ratio of C/N in their polymeric structures (Huang, Zhai, Peng, Li, & Wei, 2007).

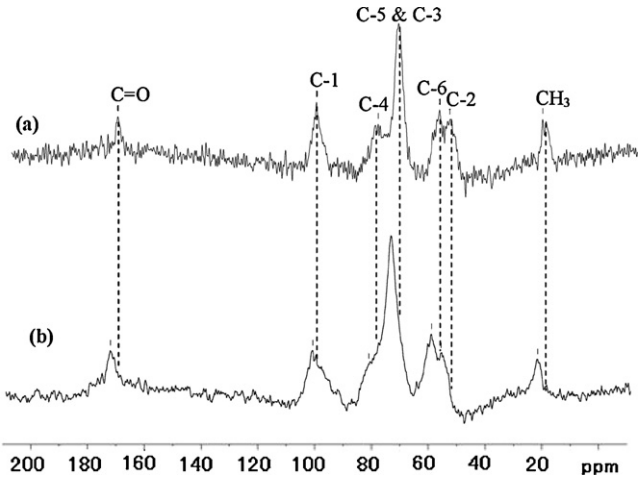

Fig. 3. ^{13}C solid state NMR spectra of (a) fresh CS-ECH film and (b) oxidized CS-ECH film.

3.1.8. ^{13}C NMR analysis

Fig. 3(a) and (b) shows the ^{13}C NMR spectra of the fresh CS-ECH film and the oxidized CS-ECH film respectively. The peaks of spectrum (a) were quite comparable to the peaks recorded by Chen, Liu, Chen, and Chen (2008), who attributed the appearance of three peaks at around 59.4, 81.1 and 102.6 ppm to the existing of —O—CH_2—CHOH—CH_2—O— linkage between the two repeated units of pyranose rings of CS. Furthermore, the peak at 172.3 ppm was attributed to the carbon atom of C=O group of acetamide (NH—CO—CH_3) residues in the N-acetyl glucosamine unit (Heux, Brugnerotto, Desbrie'res, Versali, & Rinaudo, 2000). The similarity between spectrum (a) and (b) indicates that the chemical structure of —O—CH_2—CHOH—CH_2—O— linkage remains intact during the irradiation process. In addition, the slight increase in signal at δ = 173.9 ppm can be attributed to the increase in the carbonyl (C=O) content in the polymeric structure of pyranose unit of CS. The slight shifting of the peaks in the spectrum (b) toward higher ppm values can be attributed to the new environment caused by the formation of carbonyl withdrawing functional group in the polymeric structure of the oxidized CS-ECH film.

3.1.9. FTIR analysis

The FTIR spectra of the fresh CS-ECH and the oxidized CS-ECH films are given in Supplementary Fig. 2. The 1653 cm^{-1} band can be attributed to the C=O stretching vibration in the amide group, amide I. There are observable bands at 1569 cm^{-1} (N—H bending vibration in amide group, amide II), 1418 cm^{-1} (bending vibration of primary amino group, —NH_2), and 1379 cm^{-1} (C—N bending vibration) (Ngah & Fatinathan, 2006). The characteristic bands of the saccharied structure are at 1153 cm^{-1} (asymmetrical stretching vibrations of the C—O—C glycosidic bond) (Pawlak & Mucha, 2003) and 1075 cm^{-1} (C—O stretching vibration of —COH—) (Huang et al., 2007) while bands at 1322, 1262 and 898 cm^{-1} were assigned to the asymmetrical and symmetrical stretching vibrations of the CH_2 of the pyranose ring (Ostrowska-Czubenko & Gierszewska-Druzynska, 2009; Shao, Yang, & Zhong, 2003). Appearance of a new band at 1638 cm^{-1} in spectrum (b) can be attributed to the formation of carbonyl (C=O) groups on the molecular structure of the irradiated CS-ECH film. In this regard, it has been reported that the photo-oxidation of CS caused the formation of carbonyl group which appeared as a new band ranging from 1640 to 1634 cm^{-1} (Andrady et al., 1996; Nawi et al., 2011a; Shao et al., 2003). The decrease in the band intensity of 1418 cm^{-1} can be assigned to the partial elimination of the amino groups. While, a clear increment in the band intensity of (—COH—) at 1075 cm^{-1} can be attributed

Table 1
Potentiometric titrations, swelling index, impedance and its corresponding ionic conductivity and elemental content of the fresh CS-ECH film and oxidized CS-ECH film.

Sample	Potentiometric titrations, $-NH_2$ (%)	Swelling index (%)	Impedance, R (kΩ)	Ionic conductivity, σ ($\mu S\,cm^{-1}$)	Elemental content				
					C (%)	H (%)	N (%)	C/N	C/H
Fresh CS-ECH film	70.62	36.12	146.8	0.017	39.25	6.88	7.07	5.55	5.70
Oxidized CS-ECH film	48.30	29.54	43.7	0.056	38.38	6.18	6.03	6.36	6.21

to the simultaneous replacement of amino group by the hydroxyl group at position of C-2 in the pyranose ring of CS.

3.2. Mechanistic discussion

The crosslinking reaction and the discussion of the proposed structures of the oxidized CS-ECH products **2**–**7** (structures **2**–**7**) are schematically shown in Fig. 4. The homogenous reaction of epichlorohydrine crosslinking agent with CS (structure **1**) leads to the reaction with the hydroxyl group in the primary alcohol group of CS to form the fresh crosslinked CS-ECH product **2** (structure **2**). It is known that the process of photocatalytic reaction by TiO_2 takes place after absorption of photonic energy ($h\upsilon$) that is equal or exceeds the band gap energy (E_{bg}) value for anatase which is 3.2 eV at wavelength $\lambda \leq 380$ nm. In this case, an electron (e^-) would be promoted from the valence band (VB) to the conduction band (CB) and a positive hole (h^+) would be left in the valence band, Eq. (1) (Gaya & Abdullaha, 2008).

$$TiO_2 + h\upsilon \rightarrow e^-_{CB} + h^+_{VB} \quad (1)$$

In an aqueous solution, the photolysis of water leads to the adsorption of hydroxyl ion on the catalyst surface in the dissociative form as (OH^- and H^+), Eq. (2):

$$H_2O + h\upsilon \rightarrow OH^- + H^+ \quad (2)$$

The positive hole reacts with a surface-bound hydroxyl ion to produce very powerful hydroxyl radicals (•OH), Eq. (3):

$$TiO_2\,(h^+) + OH^- \rightarrow {}^{\bullet}OH \quad (3)$$

Meanwhile, the negative electron reacts with the proton (H^+) to produce hydrogen radical (•H), Eq. (4) (Huang et al., 2007):

$$TiO_2\,(e^-) + H^+ \rightarrow {}^{\bullet}H \quad (4)$$

The •OH radicals derived from the irradiated TiO_2 surface migrates to the TiO_2/CS-ECH interface and can readily attack C-3 atom in the pyranose ring of the adjacent CS-ECH film. Unlike natural CS biopolymer, crosslinking reaction of CS with ECH leads basically to the blocking of the primary alcoholic ($-CH_2OH$) groups at position C-5 and therefore not available for oxidation.

Since, the FTIR results indicate that there is no breakage of the β-D-(1,4)-glycosidic linkages between the two repeated units of pyranose ring of CS, therefore it is postulated here that C-3 position of the pyranose ring could undergo oxidation process to yield the product **3** (structure **3**). In this respect, Ulanski and Sonntag (2000) reported the formation of a carbonyl group at C-3 when the CS solution was irradiated with γ-rays in the presence of oxygen. Generation of product **3** from **2** should follow similar oxidative radicals mechanism as previously proposed for the oxidation of CS (Nawi et al., 2011a). Product **4** (structure **4**) was then generated via partial elimination of the amino group with the simultaneous replacement by the hydroxyl groups at the position C-2. Oxidation of the other pyranose ring with simultaneous replacement of amino group by the hydroxyl group finally yielded product **6** (structure **6**). The partial elimination of the amino groups is well supported by potentiometric titration, swelling test, FTIR and CHN results which were discussed previously. Furthermore, Huang et al. (2007) reported that the partial elimination of amino group at the position of C-2 of the CS's derivative solution under γ-rays led to the simultaneous formation of the hydroxyl group at position C-2. An alternative reaction route could also possibly occur via the alternative product **5** (structure **5**) whereby both pyranose rings get oxidized. The next step involves the replacement of amino groups in both pyranose rings to form product **6**. It is also possible here that product **6** could be directly generated from further oxidation of product **3**. In this work, no evidences were obtained to suggest the formation of product **7** (structure **7**) since the $-O-CH_2-CHOH-CH_2-O-$ linkage remained intact as discussed previously in the ^{13}C NMR analysis.

3.3. Performance of the TiO_2/CS-ECH photocatalyst system for phenol removal

It was proven in our previous works that the TiO_2/oxidized-CS photocatalyst system had better photocatalytic performance than both the fresh TiO_2/CS photocatalyst system as well as the TiO_2 single layer system for the removal of phenol (Nawi et al., 2011b) and its intermediates (Jawad & Nawi, 2011). Therefore two photocatalyst systems were prepared for testing the photodegradation of phenol. First was the fresh TiO_2/CS-ECH photocatalyst system while the second system was the TiO_2/oxidized-CS-ECH photocatalyst system. In addition, a comparative study between the photocatalytic performances of TiO_2/oxidized-CS-ECH photocatalyst systems against the fresh TiO_2/CS and the TiO_2/oxidized-CS photocatalyst systems was also performed as well. The preliminary results of the photocatalytic performances of these photocatalyst systems are presented below.

3.3.1. Photocatalytic activity

Fig. 5 shows the results of the adsorption and photocatalysis tests of the different photocatalyst systems for the removal of 10 mg L^{-1} phenol at different contact times. Adsorption study was performed in order to investigate if there was any synergistic effect of the adsorption-photocatalysis or not. The calculation of the percentage of phenol remaining in the treated solution was calculated according to Eq. (5).

$$\%\,\text{of phenol remained} = \left(\frac{C_t}{C_o}\right) \times 100\% \quad (5)$$

where C_o = initial concentration of phenol before treatment ($t = 0$) (mg L^{-1}) and C_t = concentration of phenol after treatment ($t = t$) (mg L^{-1}).

As shown in Fig. 5, no adsorption of phenol was detected on the surface of all photocatalyst systems. On the other hand, after exposing the catalyst system to the light, the degradation of phenol increased with time. This meant that the degradation of phenol was mainly due to the photocatalytic process. The kinetics of phenol removal followed the pseudo-first-order kinetics shown in Supplementary Fig. 3. Both TiO_2/CS-ECH and TiO_2/oxidized-CS-ECH photocatalyst systems exhibited better photocatalytic activities than both fresh TiO_2/CS and TiO_2/oxidized-CS photocatalyst systems respectively (Fig. 5). The reason why fresh TiO_2/CS-ECH photocatalyst system shows higher photocatalytic activity than fresh TiO_2/CS photocatalyst system was due to the crosslinking treatment of CS with ECH which reinforced the chemical stability of the CS-ECH film. At this stage, no complete oxidation of

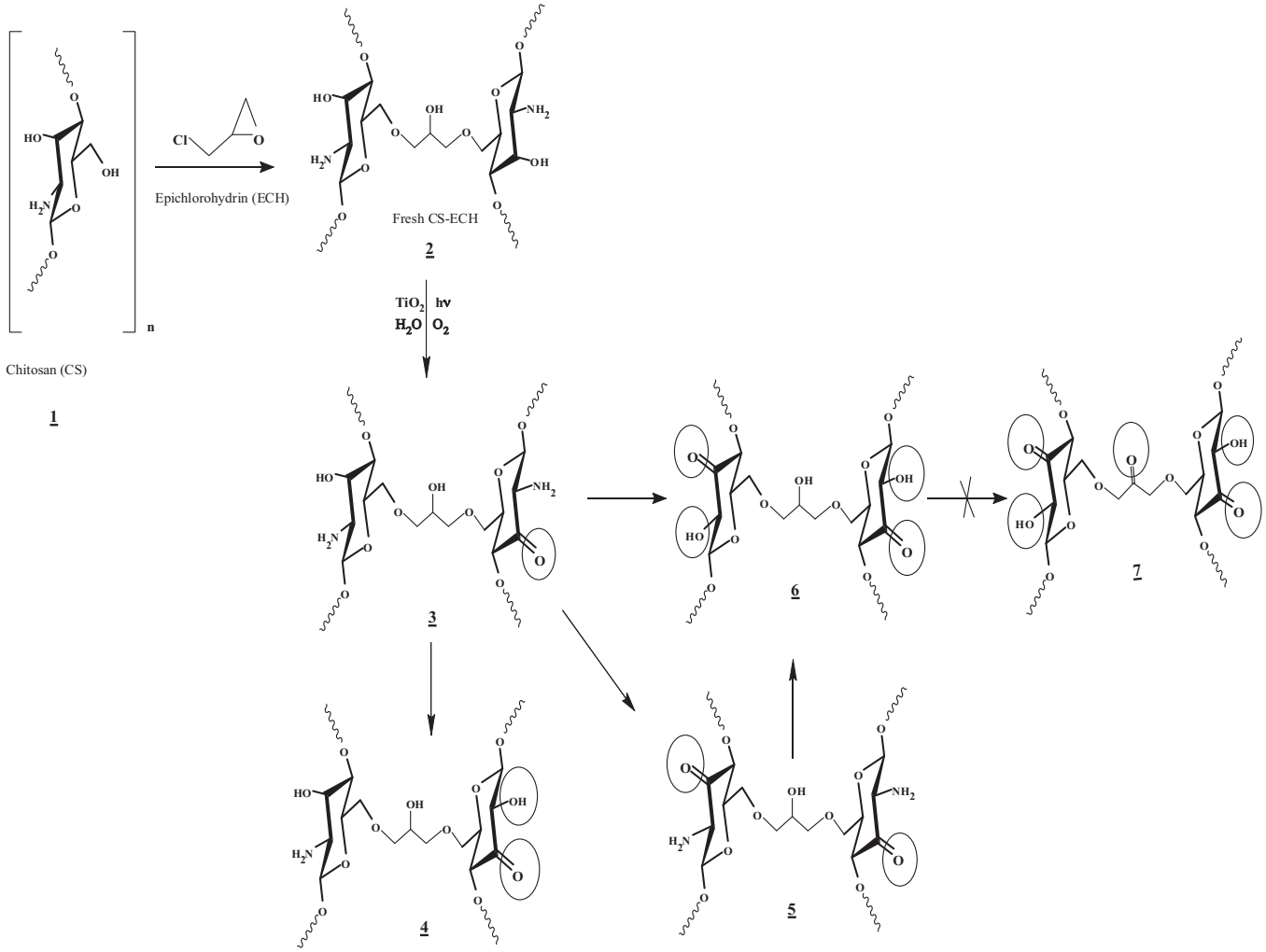

Fig. 4. Schematic representation for the homogenous crosslinking reaction of CS with ECH and the most likely structures of the oxidized CS-ECH.

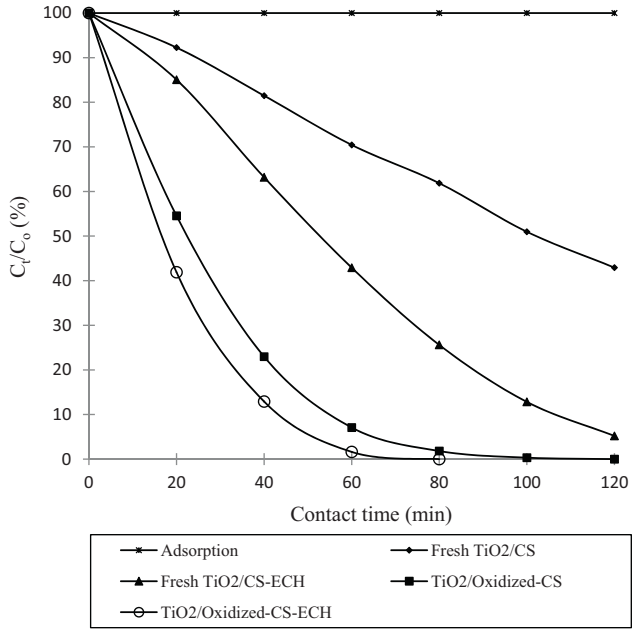

Fig. 5. Percentage of phenol remaining versus contact time (min) after photocatalytic degradation with different photocatalyst systems using a 45-W fluorescent lamp.

CS-ECH layer occurred since irradiation time was no enough to cause the oxidation of either the CS or CS-ECH films within the photocatalyst systems. In fact, the crosslinked CS-ECH is more useful in wastewater treatment technology than natural CS, since it could overcome the leaching and swelling effects normally encountered with the natural CS (Jawad & Nawi, 2011; Nawi et al., 2011a, 2011b). Furthermore, it was also observed that the TiO_2/oxidized-CS-ECH photocatalyst system had higher photocatalytic activity than the TiO_2/oxidized-CS photocatalyst system. This enhancement in the photocatalytic performance was due to the decrease in the recombination rate of the photo-induced electron–hole pairs on the surface of TiO_2 as shown in the PL spectra depicted in Fig. 6 where the PL intensity of the TiO_2/oxidized-CS-ECH was found lower than the PL intensity of the TiO_2/oxidized-CS photocatalyst system. In fact, lower PL intensity basically means better electron–hole charges separation on the surface of TiO_2 (Liqiang et al., 2006). Therefore better photocatalytic performance can be obtained by the TiO_2/oxidized-CS-ECH photocatalyst system. In fact, the presence of oxidized CS-ECH film in the photocatalyst system has a beneficial impact not only in improving the electron–hole charge separation but also on the physical strength of the oxidized CS-ECH system which has lower swelling index as compared to the swelling index of the non-crosslinked system as recorded in our previous work (Nawi et al., 2011a). Supplementary Table 1 clearly shows that the oxidized crosslinked CS-ECH has better physical strength due to lower COD values recorded upon different irradiation times.

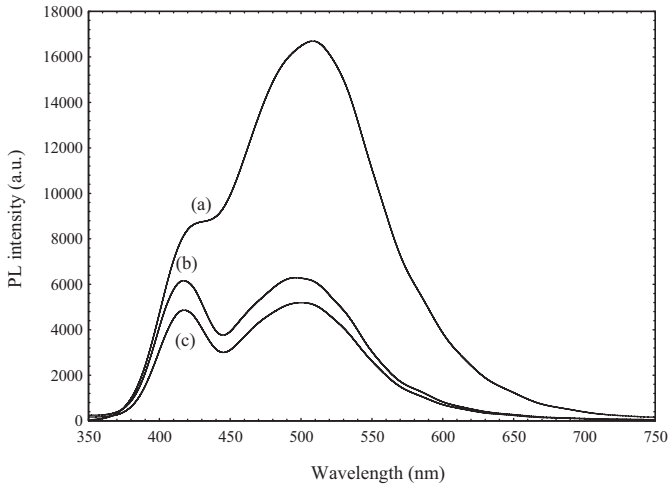

Fig. 6. Photoluminescence spectra of (a) fresh TiO_2/CS-ECH, (b) TiO_2/oxidized-CS and (c) TiO_2/oxidized-CS-ECH photocatalyst systems, at excitation wavelength of 325 nm.

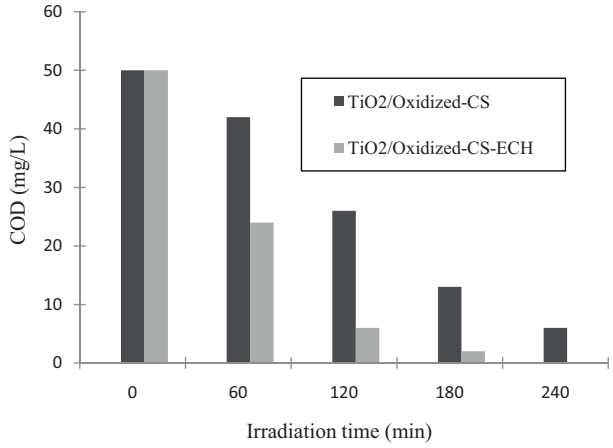

Fig. 7. COD values of 20 mg L^{-1} phenol solution upon photocatalytic degradation by TiO_2/oxidized-CS and TiO_2/oxidized-CS-ECH photocatalyst systems.

Hence, this work shows that the oxidized CS-ECH biopolymeric film is a highly viable candidate for use as a supporting biomaterial for enhancing the photocatalytic activity of the TiO_2 system, even though there is no significant contribution with respect to the adsorption of pollutants.

3.3.2. COD test

Fig. 7 shows the COD values of the treated phenol solutions versus irradiation time which were taken as a function of the mineralization rate of phenol solution into CO_2, H_2O and some sorts of mineral acids. As can be seen, the mineralization rate of phenol was generally faster by using TiO_2/oxidized-CS-ECH photocatalyst system and total mineralization can be achieved within 240 min of irradiation. On the contrary, detectable COD values were still recorded after the same time of irradiation by using TiO_2/oxidized-CS photocatalyst system. These results are in good agreement with the results of the photocatalytic activity tests, and confirm further the effectiveness of the TiO_2/oxidized-CS-ECH photocatalyst system for speeding-up the mineralization rate of phenol.

4. Conclusions

Crosslinked CS-ECH film was mildly oxidized in a very simple and environmental friendly method by using TiO_2 heterogeneous photocatalyst technology. The photocatalytic oxidation process leads to formation of the carbonyl (C=O) group, and converted CS-ECH structure into a more chemically stable form due to the partial removal of amino ($-NH_2$) and oxidation of hydroxyl (—OH) groups. The preliminary application of the oxidized CS-ECH film in heterogeneous TiO_2 photocatalyst system for water treatment technology gave a positive response for phenol removal, even though no direct adsorption of phenol was observed by the system. Most important, these results indicated that oxidized CS-ECH sensitized TiO_2 was better than the oxidized CS (Nawi et al., 2011b). Our main interest now is to study the key operational parameters governing the photocatalytic reactions of this system in the removal of phenol and other pollutants.

Acknowledgements

The authors would like to thank the Ministry of Science, Technology and Innovation (MOSTI), Malaysia for supporting this project under Science Fund Grant (305/pkimia/613402) and FRGS grant (203/pkimia/671027). We would like also to acknowledge Universiti Sains Malaysia for the USM Fellowship for funding Ali H. Jawad.

Appendix A. Supplementary data

Supplementary data associated with this article can be found, in the online version, at http://dx.doi.org/10.1016/j.carbpol.2012.04.066.

References

Andrady, A. L., Torikai, A., & Kobatake, T. (1996). Spectral sensitivity of chitosan photodegradation. *Journal of Applied Polymer Science*, *62*, 1465–1471.
Baroni, P., Vieira, R. S., Meneghetti, E., da Silva, M. G. C., & Beppu, M. M. (2008). Evaluation of batch adsorption of chromium ions on natural and crosslinked chitosan membranes. *Journal of Hazardous materials*, *152*, 1155–1163.
Blondet, F. P., Vincent, T., & Guibal, E. (2008). Hydrogenation of nitrotoluene using palladium supported on chitosan hollow fiber: Catalyst characterization and influence of operative parameters studied by experimental design methodology. *International Journal of Biological Macromolecules*, *43*, 69–78.
Chang, M. Y., & Juang, R. Y. (2004). Adsorption of tannic acid, humic acid, and dyes from water using the composite of chitosan and activated clay. *Journal of Colloid and Interface Science*, *278*, 18–25.
Chen, A. H., Liu, S. C., Chen, C. Y., & Chen, C. Y. (2008). Comparative adsorption of Cu(II), Zn(II), and Pb(II) ions in aqueous solution on the crosslinked chitosan with epichlorohydrine. *Journal of Hazardous materials*, *154*, 184–191.
Choi, W. S., Ahn, K. J., Lee, D. W., Byun, M. W., & Park, H. J. (2002). Preparation of chitosan oligomers by irradiation. *Polymer Degradation and Stability*, *78*, 533–538.
Crini, C., & Badot, P. M. (2008). Application of chitosan, a natural aminopolysaccharide, for dye removal from aqueous solution by adsorption processes using batch studies: A review of recent literature. *Progress in Polymer Science*, *33*, 399–447.
Gaya, U. I., & Abdullaha, A. H. (2008). Heterogeneous photocatalytic degradation of organic contaminants over titanium dioxide: A review of fundamentals, progress and problems. *Journal of Photochemistry and Photobiology C: Photochemistry Review*, *9*, 1–12.
Heux, L., Brugnerotto, J., Desbrie'res, J., Versali, M. F., & Rinaudo, M. (2000). Solid state NMR for determination of degree of acetylation of chitin and chitosan. *Biomacromolecules*, *1*, 746–751.
Huang, L., Zhai, M., Peng, J., Li, J., & Wei, G. (2007). Radiation-induced degradation of carboxymethylated chitosan in aqueous solution. *Carbohydrate Polymers*, *67*, 305–312.
Jawad, A. H., & Nawi, M. A. (2011). Fabrication, optimization and application of an immobilized layer-by-layer TiO_2/chitosan system for the removal of phenol and its intermediates under 45-W fluorescent lamp. *Reaction Kinetics and Catalysis Letters*, http://dx.doi.org/10.1007/s11144-011-0396-y
Kasaai, M. R. (2008). A review of several reported procedures to determine the degree of N-acetylation for chitin and chitosan using infrared spectroscopy. *Carbohydrate Polymers*, *71*, 497–508.
Kumar, M. N. R. (2000). A review of chitin and chitosan applications. *Reactive and Functional Polymers*, *46*, 1–27.
Levin, B. (2003). *Principles of forensic toxicology* (2nd ed.). USA: AACC Press., p.87
Li, Q., Su, H., & Tan, T. (2008). Synthesis of ion-imprinted chitosan-TiO_2 adsorbent and its multi-functional performances. *Biochemical Engineering Journal*, *38*, 212–218.
Liqiang, J., Yichun, Q., Baiqi, W., Shudan, L., Baojiang, J., Libin, Y., Wei, F., Honggang, F., & Jiazhong, S. (2006). Review of photoluminescence performance of nano-sized semiconductor materials and its relationships with photocatalytic activity. *Solar Energy Materials and Solar Cells*, *90*, 1773–1787.

Mi, F. L., Shya, S. S., Wu, Y. B., Lee, S. T., Shyong, J. Y., & Huang, R. N. (2001). Fabrication and characterization of a sponge-like asymmetric chitosan membrane as a wound dressing. *Biomaterials*, *22*, 165–173.

Nagasawa, N., Mitomo, H., Yoshii, F., & Kume, T. (2000). Radiation-induced degradation of sodium alginate. *Polymer Degradation and Stability*, *69*, 279–285.

Nawi, M. A., Jawad, A. H., Sabar, S., & Ngah, W. S. W. (2011a). Photocatalytic-oxidation of solid state chitosan by immobilized bilayer assembly of TiO_2–chitosan under a compact household fluorescent lamp irradiation. *Carbohydrate Polymers*, *83*, 1146–1152.

Nawi, M. A., Jawad, A. H., Sabar, S., & Ngah, W. S. W. (2011b). Immobilized bilayer TiO_2/chitosan system for the removal of phenol under irradiation by a 45 Watt compact fluorescent lamp. *Desalination*, *280*, 288–296.

Nawi, M. A., Sabar, S., Jawad, A. H., & Ngah, W. S. W. (2010). Adsorption of Reactive Red 4 by immobilized chitosan on glass plates: Towards the design of immobilized TiO_2–chitosan synergistic photocatalyst-adsorption bilayer system. *Biochemical Engineering Journal*, *49*, 317–325.

Ngah, W. S. W., & Fatinathan, S. (2006). Chitosan flakes and chitosan–GLA beads for adsorption of *p*-nitrophenol in aqueous solution. *Journal of Colloid and Interface Science*, *277*, 214–222.

Ngah, W. S. W., Endud, C. S., & Mayanar, R. (2002). Removal of copper(II) ions from aqueous solution onto chitosan and cross-linked chitosan beads. *Reactive and Functional Polymers*, *50*, 181–190.

Ngah, W. S. W., Ghani, S. A., & Hoon, L. L. (2002). Comparative adsorption of lead(II) on flake and bead-type of chitosan. *Journal of the Chinese Chemical Society*, *49*, 625–628.

Ostrowska-Czubenko, J., & Gierszewska-Druzynska, M. (2009). Effect of ionic crosslinking on the water state in hydrogel chitosan membranes. *Carbohydrate Polymers*, *77*, 590–598.

Pawlak, A., & Mucha, M. (2003). Thermogravimetric and FTIR studies of chitosan blends. *Thermochimica Acta*, *396*, 153–166.

Rodrigues, I. R., Forte, M. M. C., Azambuja, D. S., & Castagno, K. R. L. (2007). Synthesis and characterization of hybrid polymeric networks (HPN) based on polyvinyl alcohol/chitosan. *Reactive and Functional Polymers*, *67*, 708–715.

Shao, J., Yang, Y., & Zhong, Q. (2003). Studies on preparation of oligoglucosamine by oxidative degradation under microwave irradiation. *Polymer Degradation and Stability*, *82*, 395–398.

Ulanski, P., & Sonntag, C. V. (2000). OH-radical-induced chain scission of chitosan in the absence and presences of dioxygen. *Journal of the Chemical Society, Perkin Transactions*, *2*, 2022–2028.

Vieira, R. S., & Beppu, M. M. (2006). Interaction of natural and cross-linked chitosan membranes with Hg(II) ions. *Colloids and Surfaces A: Physicochemical and Engineering Aspects*, *279*, 196–207.

Wan, Y., Creber, K. A. M., Peppley, B., & Bui, V. T. (2003). Ionic conductivity and related properties of crosslinked chitosan membranes. *Journal of Applied Polymer Science*, *89*, 306–317.

Wang, S. M., Huang, Q. Z., & Wang, Q. S. (2005). Study on the synergetic degradation of chitosan with ultraviolet light and hydrogen peroxide. *Carbohydrate Research*, *340*, 1143–1147.

Zainal, Z., Hui, L. K., Hussein, M. Z., Abdullah, A. H., & Hamadneh, I. R. (2009). Characterization of TiO_2–chitosan/glass photocatalyst for the removal of a monoazo dye via photodegradation-adsorption process. *Journal of Hazardous materials*, *164*, 138–145.

Zainol, I., Akil, H. M., & Mastor, A. (2009). Effect of γ-irradiation on the physical and mechanical properties of chitosan powder. *Materials Science and Engineering C*, *29*, 292–297.

Zubieta, C. E., Messina, P. V., Luengo, C., Dennehy, M., Pieroni, O., & Schulz, P. C. (2008). Reactive dyes remotion by porous TiO_2–chitosan materials. *Journal of Hazardous materials*, *152*, 765–777.